Terahertz-Field-Induced Time Shifts in Atomic Photoemission

Georg Schmid,[1,*] Kirsten Schnorr,[1,†] Sven Augustin,[1] Severin Meister,[1] Hannes Lindenblatt,[1] Florian Trost,[1] Yifan Liu,[1] Nikola Stojanovic,[2] Alaa Al-Shemmary,[2] Torsten Golz,[2] Rolf Treusch,[2] Michael Gensch,[3] Matthias Kübel,[4,5] Lutz Foucar,[6] Artem Rudenko,[7] Joachim Ullrich,[8] Claus Dieter Schröter,[1] Thomas Pfeifer,[1] and Robert Moshammer[1,‡]

[1]*Max-Planck-Institut für Kernphysik, Saupfercheckweg 1, D-69117 Heidelberg, Germany*
[2]*Deutsches Elektronen-Synchrotron (DESY), Notkestraße 85, D-22607 Hamburg, Germany*
[3]*Helmholtz-Zentrum Dresden-Rossendorf, Bautzner Landstraße 400, D-01328 Dresden, Germany*
[4]*Department of Physics, Ludwig-Maximilians-Universität München, D-85748 Garching, Germany*
[5]*Max-Planck-Institut für Quantenoptik, Hans-Kopfermann-Straße 1, D-85748 Garching, Germany*
[6]*Max-Planck-Institut für medizinsche Forschung, Jahnstraße 29, D-69120 Heidelberg, Germany*
[7]*Kansas State University, 116 Cardwell Hall, Manhattan, Kansas 66506, USA*
[8]*Physikalisch-Technische Bundesanstalt (PTB), Bundesallee 100, D-38116 Braunschweig, Germany*

(Received 9 September 2018; published 19 February 2019)

Time delays for atomic photoemission obtained in streaking or reconstruction of attosecond bursts by interference of two-photon transitions experiments originate from a combination of the quantum mechanical Wigner time and the Coulomb-laser coupling. While the former was investigated intensively theoretically as well as experimentally, the latter attracted less interest in experiments and has mostly been subject to calculations. Here, we present a measurement of the Coulomb-laser coupling-induced time shifts in photoionization of neon at 59.4 eV using a terahertz (THz) streaking field ($\lambda = 152$ μm). Employing a reaction microscope at the THz beamline of the free-electron laser in Hamburg (FLASH), we have measured relative time shifts of up to 70 fs between the emission of $2p$ photoelectrons (~38 eV) and low-energetic (<1 eV) photoelectrons. A comparison with theoretical predictions on Coulomb-laser coupling reveals reasonably good agreement.

DOI: 10.1103/PhysRevLett.122.073001

Photoionization has been investigated for decades; however, the question of whether the emission of the electron occurs instantaneously in time or with a *delay* relative to the photoabsorption remains a subject of controversy. With the development of *attosecond science* [1,2], the observation of photoionization on its natural timescale came into reach. In this regard, light-field-driven electron streaking [3], which uses extreme-ultraviolet (XUV) attosecond pulses as pump and few-cycle phase-controlled infrared (IR) fields as a probe, has been demonstrated to resolve electronic dynamics on the subfemtosecond level [4–6]. The basic idea is that an electron emerging in photoionization experiences a momentum shift that, in the first approximation, is proportional to the strength of the vector potential of the probe field at the moment when the electron reaches the ionization continuum. Following this approach, Schultze *et al.* [6] reported a delayed emission of $2p$ relative to $2s$ photoelectrons in neon of (21 ± 5) as, which stimulated an intense debate about the origins and the exact values of time shifts in atomic photoemission (see, e.g., Refs. [7–25]). Only recently, this controversy was resolved by pointing out the importance of shake-up processes [26].

In the course of investigating time shifts in atomic photoemission, it was shown that besides the quantum mechanical Eisenbud-Wigner-Smith (EWS) time [27–29], which is typically on the order of a few attoseconds, the total measured time shifts always go along with measurement-induced contributions due to the coupling between the atomic Coulomb and the probing laser field [30].

Analytical expressions accounting for Coulomb-laser coupling (CLC) were derived [11,15,18], and it was shown that these are in very good agreement with time-dependent quantum calculations and classical trajectory Monte Carlo simulations [15,18]. In contrast to EWS, it is predicted that CLC does not depend on the specific atomic target [17]. This universality allows accessing EWS time shifts alone by correcting the measured time shifts for CLC [31].

In contrast to most previous studies that aimed to measure EWS time shifts [6,26,31–33], the present experiment measures CLC and thus allows benchmarking theoretical predictions based on analytical expressions. The CLC time shifts from Refs. [11,15,18] depend on the energy E of the outgoing electron and the wavelength of the probe field λ and share the following proportionality:

$$t_{\mathrm{clc}}(E,\lambda) \propto -\frac{1}{E^{3/2}} \ln(4E\lambda). \tag{1}$$

According to Eq. (1), CLC is more pronounced for long wavelengths of the probe field and low-energetic photoelectrons. Both conditions are fulfilled in the present experiment. Instead of an IR probe field ($\lambda_{\mathrm{IR}} = 800$ nm), which is usually used in attosecond streaking [34,35], we employ a terahertz (THz) probe field with a factor of 200 longer wavelength ($\lambda_{\mathrm{THz}} = 152$ μm). Low-energetic photoelectrons arise from photoionization accompanied by a shake-up of the residual neon ion [in the following called shake-up (su) photoelectrons]. At a photon energy of $\hbar\omega_{\mathrm{xuv}} = 59.4$ eV, $\mathrm{Ne}^{+}(1s^2 2s^2 2p^4 nl)$ shake-up satellite states lying just below the double-ionization threshold at 62.5 eV are excited [36], and the su photoelectrons created in the process

$$\mathrm{Ne}(1s^2 2s^2 2p^6) + \hbar\omega_{\mathrm{xuv}}(59.4\ \mathrm{eV}) \rightarrow \mathrm{Ne}^{+}(1s^2 2s^2 2p^4 nl) + e^{-}_{su} \quad (2)$$

have low kinetic energies (<1 eV).

The experiment was carried out at the XUV free-electron laser in Hamburg (FLASH) [37], which has an undulator-based THz beamline [38]. The XUV and the THz pulses are generated by the same electron bunch in two different undulators and thus are intrinsically synchronized [39]. The effective pulse repetition rate was 600 pulses/s. The XUV intensity was kept low at $\sim 10^{10}$ W/cm^2 in the interaction region. An overview of the experimental setup is shown in Fig. 1(a). The XUV beam is focused down to a diameter of approximately 100 μm by a Mo/Si multilayer mirror, whereas the THz beam is brought into focus by a paraboloidal copper mirror. A large THz focus of about 1 mm diameter ensures that all photoelectrons are ejected into a homogeneous probe field. Following the approach from Ref. [40], the average XUV pulse duration is estimated to be $\tau_{\mathrm{xuv}} = (150 \pm 50)$ fs (FWHM). With a half period of the THz-probe field of $T_{\mathrm{THz}}/2 = 253$ fs, the streaking condition $\tau_{\mathrm{xuv}} < T_{\mathrm{THz}}/2$ is fulfilled. The XUV and the THz beam are focused into a supersonic gas jet containing the target neon atoms. The emerging ions and electrons are detected by means of a reaction microscope (REMI) [41]. Full 4π acceptance for the photoelectrons is achieved by superimposing an electric (18.6 V/cm) and a magnetic field (15.5 G). Measuring the time-of-flight and impact position of ions and electrons on the REMI detectors allows reconstructing their initial three-dimensional momentum vectors. The relative arrival time Δt between the XUV and the THz pulse was adjusted in steps of 1 fs (total range, $\pm$1000 fs) by moving the XUV mirror with a piezo stage [cf. Fig. 1(a)].

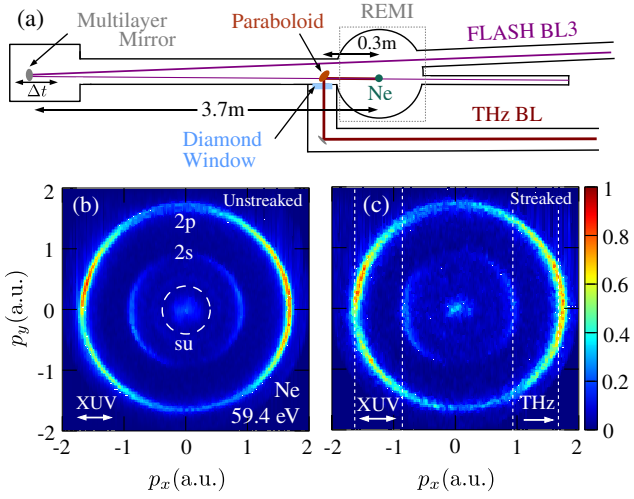

FIG. 1. (a) Overview of the REMI setup at FLASH. (b) Neon photoelectron momentum distribution at 59.4 eV in the plane including the FEL polarization axis (along p_x) and the FEL beam axis (along p_y). The rings of constant radius are assigned to $2p$ and $2s$ photoelectrons. The distribution around the origin is attributed to su photoelectrons [cf. Eq. (2)]. (c) Momentum distribution for the maximum positive shift $+\Delta p_{x,\mathrm{max}}$ in the presence of the THz probe (polarized along p_x). The dashed vertical lines indicate the initial unstreaked momenta of $2p$ and $2s$ photoelectrons.

First, the interaction of the XUV beam with neon in the absence of the THz probe field is studied. Figure 1(b) shows the corresponding photoelectron momentum distribution. For this plot, only electrons that are emitted in a plane including the FEL polarization axis (along p_x) and the FEL beam axis (along p_y) are selected by a condition on the p_z momentum component ($-0.35 < p_z < +0.35$ a.u.). In this representation, rings of constant radius correspond to photoelectrons with one particular energy. The ring of radius $p_{2p} = 1.67$ a.u. is attributed to $2p$ photoelectrons (binding energy $E_{b,2p} = 21.56$ eV [42]). The dipolelike structure of radius $p_{2s} = 0.90$ a.u. is assigned to $2s$ photoelectrons (binding energy $E_{b,2s} = 48.48$ eV [36]). The ratio of the measured absolute yields for $2s$ and $2p$ ionization [$R_{2s/2p} = (8 \pm 1)\%$] agrees well with theory ($R^{\mathrm{calc}}_{2s/2p} = 7.7\%$ [43]). Besides these features, an isotropic distribution is visible around the origin in Fig. 1(b) that is assigned to su photoelectrons [cf. Eq. (2)]. The su photoelectrons are selected by a condition on the total momentum [$0 < p_{\mathrm{tot},su} = (p_x^2 + p_y^2 + p_z^2)^{1/2} < 0.35$ a.u.]. They have a mean energy of 0.8 eV, and thus the mean binding energy of the $\mathrm{Ne}^{+}(1s^2 2s^2 2p^4 nl)$ shake-up satellite states [cf. Eq. (2)] is $E_{b,su} = \hbar\omega_{\mathrm{xuv}} - 0.8$ eV $= 58.6$ eV. The electron energy resolution is limited by the XUV bandwidth of 0.7 eV (FWHM) and the resolution of our electron spectrometer [$\sim$0.1 eV (FWHM)]. Therefore, we measure a su photoelectron spectrum that includes contributions from several satellite states [44]. The yield ratio between su and $2s$ photoelectrons [$R_{su/2s} = (11 \pm 2)\%$] agrees with synchrotron measurements [45]. Contributions from autoionizing doubly excited states are not expected, as the present photon energy does not match the respective excitation energies [46].

After having identified the structure of the photoelectron spectrum, we turn to the results obtained in the presence of the THz-probe field. Neglecting CLC, the momentum shift $\Delta\mathbf{p}(t) = -e\mathbf{A}(t)$ that an electron experiences due to the streaking probe field [with vector potential $\mathbf{A}(t)$] adds to the initial momentum $\mathbf{p}_0$ of the electron: $\mathbf{p}(t) = \mathbf{p}_0 + \Delta\mathbf{p}(t)$ [3]. The photoelectron momentum distribution along the THz polarization direction is displayed in Fig. 1(c) for the case of maximum positive shift $+\Delta p_{x,\max}$. The yield ratio $R_{su/2p}$ is the same as for the measurement with XUV only, and for both cases no double ionization of Ne is observed.

The momentum component p_x is shown as a function of the pump-probe delay in Fig. 2(a). Here, only electrons that are predominantly emitted along the THz polarization axis, i.e., along p_x, are selected by the conditions $-0.35 < p_y < +0.35$ a.u. and $-0.35 < p_z < +0.35$ a.u. A delay-dependent oscillation of p_x is observed for all photoelectrons. For a quantitative analysis, the scatter histogram in Fig. 2(a) is transformed into profile plots. To this end, the $2p$, $2s$, and su photoelectrons are selected by cuts on their total momentum ($1.45 < |p_{\mathrm{tot},2p}| < 1.90$ a.u., $0.80 < |p_{\mathrm{tot},2s}| < 1.07$ a.u., and $0 < p_{\mathrm{tot},su} < 0.35$ a.u.). For each selection, the mean value of p_x is computed for every bin of the delay axis. The resulting offset-corrected profiles $\Delta p(t)$ are fitted by a sinusoidal function $\Delta p(t) = p_{\max}\sin(2\pi f_{\mathrm{THz}} t + \varphi)$ with amplitude $p_{\max}$, frequency f_{THz}, and phase φ [cf. Figs. 2(b) and 2(c)]. The fit to the $2p$ photoelectrons gives $f_{\mathrm{THz}} = (1.975 \pm 0.004)$ THz and $p_{\max} = (0.04 \pm 0.01)$ a.u., which corresponds to a field strength of $E_{\mathrm{THz}} = (6.2 \pm 1.5) \times 10^6$ V/m.

The relative time shifts in the emission of $2p$, $2s$, and su photoelectrons are encoded in the phase shifts of the corresponding streaking traces [6]. $2p$ and $2s$ photoelectrons are compared in Fig. 2(b). An enlargement between -50 and 220 fs shows no phase shift [cf. Fig. 2(d)]. The data evaluation is extended by also analyzing the streaking traces of two further representations of the momentum shift, i.e., $\Delta p_{\mathrm{tot}}(t)$ and $\Delta p_x(t)$ without restricting conditions on p_y and p_z. Finally, a mean value of $\Delta\langle t\rangle_{2p-2s} = (2.0 \pm 3.8)$ fs is obtained. This result does not allow us to draw a conclusion on a relative time shift between the emission of $2s$ and $2p$ photoelectrons. In contrast to attosecond streaking experiments, which achieve temporal resolutions of a few attoseconds [6], the measurement of EWS or CLC time shifts [$t_{2p}^{\mathrm{clc}}(E = 37.8\ \mathrm{eV}) \approx 40$ as and $t_{2s}^{\mathrm{clc}}(E = 10.9\ \mathrm{eV}) \approx 200$ as [47]] is precluded by the limited resolution of the present measurement with long-wavelength streaking.

As a relative time shift in the emission of $2p$ and $2s$ could not be resolved, su photoelectrons are exclusively compared to $2p$ photoelectrons. Fits to the $\Delta p_x(t)$ profiles of $2p$ and su photoelectrons are displayed in Figs. 2(c) and 2(e). A relative phase shift between the fits to the $2p$ and su photoelectrons is visible as a horizontal offset along $\Delta p_x = 0$ [cf. Fig. 2(e)].

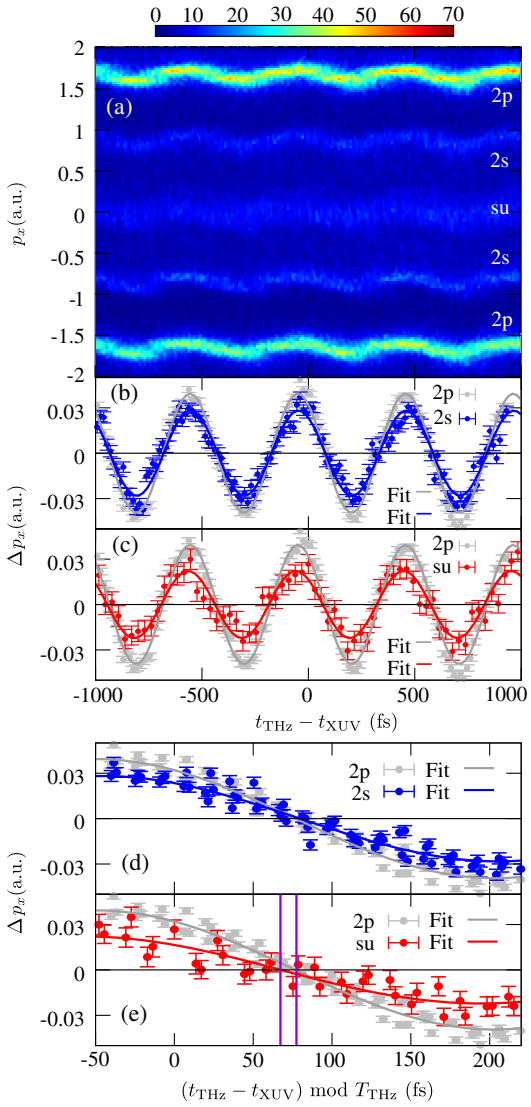

FIG. 2. (a) Delay-dependent momentum p_x for $2p$, $2s$, and su photoelectrons. Only electrons that fulfill the conditions $-0.35 < p_y < +0.35$ a.u. and $-0.35 < p_z < +0.35$ a.u. are plotted. (b) Δp_x as a function of delay with the same momentum conditions as (a) for $2p$ (gray dots) and $2s$ (blue dots) photoelectrons. The gray and blue lines are fits $\Delta p_x(t) = p_{\max}\sin(2\pi f_{\mathrm{THz}} t + \varphi)$ for $2p$ and $2s$ photoelectrons, respectively. For fitting, the frequency $f_{\mathrm{THz}} = 1.975$ THz is fixed. (c) The same as (b), but for $2p$ (gray dots and line) and su (red dots and line) photoelectrons (selected by $0 < p_{\mathrm{tot},su} < 0.35$ a.u.). (d) Enlargement of (b) for delays ranging from -50 to 220 fs. (e) The same range as (d), but the delay is plotted modulo the period of the THz field. The purple lines indicate a relative time shift visible in the horizontal offset of the zero crossings of the fits.

According to Eq. (1), CLC depends on the probe-field wavelength and the energy of the photoelectron. However, the relative time shift $\Delta t_{2p-su}(E)$ cannot be retrieved for

distinct photoelectron energies in the present experiment. The measured energy represents an average over several *su* photoelectron energies ($\langle E_{su} \rangle = 0.78$ eV) defined by the selecting momentum condition ($0 < p_{\mathrm{tot},su} < 0.35$ a.u.). Moreover, the measured energy is always a superposition of the initial energy and the energy gained in the streaking field. The two contributions cannot be disentangled, as just the final streaked energy is measured.

In order to still track $\Delta t_{2p-su}(E)$ in the experiment, the momentum condition $0 < p_{\mathrm{tot},su} < p^{\mathrm{max}}_{\mathrm{tot},su}$, which is used to select the *su* photoelectrons, is varied. This way, one is able to "tune" the mean energy of the streaked *su* photoelectrons by choosing electrons that are less or more energetic. For each selection, Δt_{2p-su} is retrieved in analogy to Fig. 2(c) and the corresponding mean photoelectron energy is determined. The outcome of this analysis is plotted in Fig. 3(d).

To compare the experimental data to theoretical CLC predictions, we employ a classical simulation which uses the set of *su* photoelectrons obtained in the measurement with XUV only [cf. Fig. 1(b)] as input. For each of these unstreaked photoelectrons, we determine its kinetic energy E and the expected CLC time shift $t_{\mathrm{clc}}(E)$ using the analytical formulas [48] from Refs. [11,15,18]. Then, the individual photoelectron momentum component p_x^0 along the streaking axis is modified according to

$$p_x^{\mathrm{sim}}(t) = p_x^0 + p_{\mathrm{max}} \sin\{2\pi f_{\mathrm{THz}}[t + t_{\mathrm{clc}}(E)]\}. \quad (3)$$

The obtained, simulated momentum distribution of *su* photoelectrons, which is now a function of the delay, is shown in Fig. 3(a) using the CLC expression from Ref. [11] for photoelectrons $0 < p_{\mathrm{tot},su} < 0.35$ a.u. Figures 3(b) and 3(c) display the phase-shift analysis on the simulated data for *su* and $2p$ photoelectrons in analogy to Figs. 2(c) and 2(e). In order to determine $\Delta t^{\mathrm{sim}}_{2p-su}(E)$, the simulated data are analyzed in exactly the same way as the experimental data with THz streaking; i.e., the momentum condition $0 < p_{\mathrm{tot},su} < p^{\mathrm{max}}_{\mathrm{tot},su}$ is varied as well, and for each selection the mean energy of the streaked photoelectrons is determined.

A comparison between the measurement (black dots) and simulation (green head-down triangles, orange squares, and blue head-up triangles) is shown in Fig. 3(d). For low photoelectron energies, the relative time shift increases. Although the theoretical curves are not in perfect agreement with the experiment, the overall trend is well reproduced. The flattening of the experimental data compared to theory at energies $E < 0.35$ eV is presumed to originate from the diverging character of the long-range Coulomb component of the EWS time for small photoelectron energies. According to Ref. [15], the corresponding time shift is about +30 fs for $E = 0.2$ eV, which is comparable to the values shown in Fig. 3(d). Towards larger energies, the EWS contribution decreases considerably, being smaller than +5 fs for $E > 0.5$ eV.

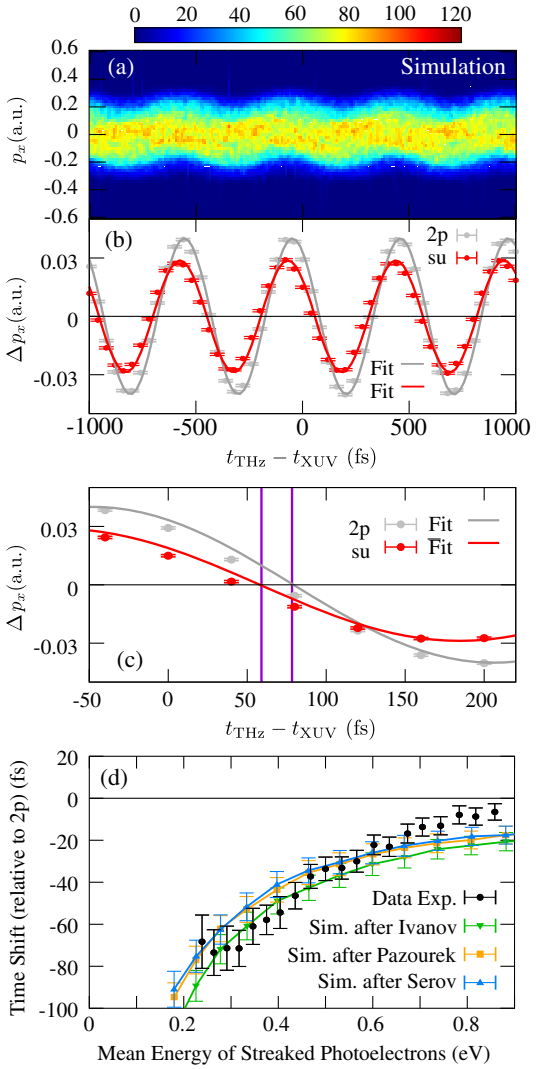

FIG. 3. (a) Simulation of p_x vs delay for *su* photoelectrons with $0 < p_{\mathrm{tot},su} < 0.35$ a.u. using the CLC formula from Ref. [11]. (b) Δp_x as a function of delay extracted from (a) for *su* (red dots) and $2p$ photoelectrons (gray dots). The red and gray lines are sinusoidal fits $\Delta p_x(t) = p_{\mathrm{max}} \sin(2\pi f_{\mathrm{THz}} t + \varphi)$ for *su* and $2p$ photoelectrons, respectively. (c) Enlargement of (b) for delays ranging from −50 to 220 fs. The purple lines indicate a relative phase shift. (d) Time shift Δt_{2p-su} of *su* relative to $2p$ photoelectrons as a function of the mean energy of the streaked *su* photoelectrons.

At large photoelectron energies, time differences of a few to tens of attoseconds at most between the ground and shake-up states were reported for helium [49] and neon [26], respectively. Therefore, it seems very unlikely that an EWS contribution due to electron-electron correlation during the shake-up process is responsible for the mismatch between the experiment and theory in Fig. 3(d), where $|\Delta t^{\mathrm{exp}}_{2p-su}(0.8\ \mathrm{eV}) - \Delta t^{\mathrm{sim}}_{2p-su}(0.8\ \mathrm{eV})| \approx 10$ fs.

In summary, we studied time shifts in XUV photoemission from neon atoms at 59.4 eV using a reaction microscope at FLASH and a THz streaking field ($\lambda = 152$ μm). We measured energy-dependent time shifts up to 70 fs in the emission of photoelectrons from shake-up ionization and direct $2p$ photoelectrons. The experimental results are in good agreement with simulations accounting for CLC-induced time shifts in atomic photoemission. This way, we experimentally confirm the universality and validity level of quasiclassically derived analytical formulas accounting for CLC. This is of crucial importance to undoubtedly disentangle CLC and EWS time shift contributions in, e.g., attosecond streaking experiments.

We thank the entire FLASH team including the accelerator, photon diagnostics, and beam line staff. C. Kaiser and B. Knape from the MPIK Heidelberg are acknowledged for their technical support. K. S. was funded by a Peter Paul Ewald Fellowship from the Volkswagen Foundation. A. R. was supported by the Chemical Sciences, Geosciences, and Biosciences Division, Office of Basic Energy Sciences, Office of Science, U.S. Department of Energy under Award No. DEFG02-86ER13491.

*georg.schmid@mpi-hd.mpg.de
†Present address: Paul Scherrer Institut, CH-5232 Villigen PSI, Switzerland.
‡robert.moshammer@mpi-hd.mpg.de

[1] A. Scrinzi, M. Yu. Ivanov, R. Kienberger, and D. M. Villeneuve, J. Phys. B **39**, R1 (2006).
[2] P. B. Corkum and F. Krausz, Nat. Phys. **3**, 381 (2007).
[3] J. Itatani, F. Quéré, G. L. Yudin, M. Yu. Ivanov, F. Krausz, and P. B. Corkum, Phys. Rev. Lett. **88**, 173903 (2002).
[4] M. Drescher, M. Hentschel, R. Kienberger, M. Uiberacker, V. Yakovlev, A. Scrinzi, Th. Westerwalbesloh, U. Kleineberg, U. Heinzmann, and F. Krausz, Nature (London) **419**, 803 (2002).
[5] A. L. Cavalieri, N. Müller, Th. Uphues, V. S. Yakovlev, A. Baltuška, B. Horvath, B. Schmidt, L. Blümel, R. Holzwarth, and S. Hendel *et al.*, Nature (London) **449**, 1029 (2007).
[6] M. Schultze, M. Fieß, N. Karpowicz, J. Gagnon, M. Korbman, M. Hofstetter, S. Neppl, A. L. Cavalieri, Y. Komninos, and Th. Mercouris *et al.*, Science **328**, 1658 (2010).
[7] O. Smirnova, M. Spanner, and M. Yu. Ivanov, J. Phys. B **39**, S323 (2006).
[8] O. Smirnova, A. S. Mouritzen, S. Patchkovskii, and M. Yu. Ivanov, J. Phys. B **40**, F197 (2007).
[9] C.-H. Zhang and U. Thumm, Phys. Rev. A **82**, 043405 (2010).
[10] A. S. Kheifets and I. A. Ivanov, Phys. Rev. Lett. **105**, 233002 (2010).
[11] M. Yu. Ivanov and O. Smirnova, Phys. Rev. Lett. **107**, 213605 (2011).
[12] S. Nagele, R. Pazourek, J. Feist, K. Doblhoff-Dier, Ch. Lemell, K. Tőkési, and J. Burgdörfer, J. Phys. B **44**, 081001 (2011).
[13] C.-H. Zhang and U. Thumm, Phys. Rev. A **84**, 033401 (2011).
[14] L. R. Moore, M. A. Lysaght, J. S. Parker, H. W. van der Hart, and K. T. Taylor, Phys. Rev. A **84**, 061404 (2011).
[15] R. Pazourek, S. Nagele, and J. Burgdörfer, Faraday Discuss. **163**, 353 (2013).
[16] J. M. Dahlström, A. L'Huillier, and A. Maquet, J. Phys. B **45**, 183001 (2012).
[17] J. M. Dahlström, D. Guénot, K. Klünder, M. Gisselbrecht, J. Mauritsson, A. L'Huillier, A. Maquet, and R. Taïeb, Chem. Phys. **414**, 53 (2013).
[18] V. V. Serov, V. L. Derbov, and T. A. Sergeeva, Phys. Rev. A **87**, 063414 (2013).
[19] J. Feist, O. Zatsarinny, S. Nagele, R. Pazourek, J. Burgdörfer, X. Guan, K. Bartschat, and B. I. Schneider, Phys. Rev. A **89**, 033417 (2014).
[20] A. Maquet, J. Caillat, and R. Taïeb, J. Phys. B **47**, 204004 (2014).
[21] L. Torlina, F. Morales, J. Kaushal, I. Ivanov, A. Kheifets, A. Zielinski, A. Scrinzi, H. G. Muller, S. Sukiasyan, M. Ivanov, and O. Smirnova, Nat. Phys. **11**, 503 (2015).
[22] R. Pazourek, S. Nagele, and J. Burgdörfer, J. Phys. B **48**, 061002 (2015).
[23] L. Cattaneo, J. Vos, M. Lucchini, L. Gallmann, C. Cirelli, and U. Keller, Opt. Express **24**, 29060 (2016).
[24] A. S. Kheifets, A. W. Bray, and I. Bray, Phys. Rev. Lett. **117**, 143202 (2016).
[25] L. Argenti, Á. Jiménez-Galán, J. Caillat, R. Taïeb, A. Maquet, and F. Martín, Phys. Rev. A **95**, 043426 (2017).
[26] M. Isinger, R. J. Squibb, D. Busto, S. Zhong, A. Harth, D. Kroon, S. Nandi, C. L. Arnold, M. Miranda, J. M. Dahlström, E. Lindroth, R. Feifel, M. Gisselbrecht, and A. L'Huillier, Science **358**, 893 (2017).
[27] L. Eisenbud, Ph.D. thesis, Princeton University, 1948.
[28] E. P. Wigner, Phys. Rev. **98**, 145 (1955).
[29] F. T. Smith, Phys. Rev. **118**, 349 (1960).
[30] In the literature referred to as Coulomb-laser coupling [7,8,12] or continuum-continuum interaction [16].
[31] C. Palatchi, J. M. Dahlström, A. S. Kheifets, I. A. Ivanov, D. M. Canaday, P. Agostini, and L. F. DiMauro, J. Phys. B **47**, 245003 (2014).
[32] K. Klünder, J. M. Dahlström, M. Gisselbrecht, T. Fordell, M. Swoboda, D. Guénot, P. Johnsson, J. Caillat, J. Mauritsson, A. Maquet *et al.*, Phys. Rev. Lett. **106**, 143002 (2011).
[33] D. Guénot, K. Klünder, C. L. Arnold, D. Kroon, J. M. Dahlström, M. Miranda, T. Fordell, M. Gisselbrecht, P. Johnsson, J. Mauritsson *et al.*, Phys. Rev. A **85**, 053424 (2012).
[34] R. Kienberger, E. Goulielmakis, M. Uiberacker, A. Baltuska, V. Yakovlev, F. Bammer, A. Scrinzi, Th. Westerwalbesloh, U. Kleineberg, U. Heinzmann, M. Drescher, and F. Krausz, Nature (London) **427**, 817 (2004).
[35] E. Goulielmakis, M. Uiberacker, R. Kienberger, A. Baltuska, V. Yakovlev, A. Scrinzi, Th. Westerwalbesloh, U. Kleineberg, U. Heinzmann, M. Drescher, and F. Krausz, Science **305**, 1267 (2004).

[36] A. Kikas, S. J. Osborne, A. Ausmees, S. Svensson, O.-P. Sairanen, and S. Aksela, J. Electron Spectrosc. Relat. Phenom. **77**, 241 (1996).
[37] K. Tiedtke *et al.*, New J. Phys. **11**, 023029 (2009).
[38] M. Gensch *et al.*, Infrared Phys. Technol. **51**, 423 (2008).
[39] N. Stojanovic and M. Drescher, J. Phys. B **46**, 192001 (2013).
[40] U. Frühling, M. Wieland, M. Gensch, T. Gebert, B. Schütte, M. Krikunova, R. Kalms, F. Budzyn, O. Grimm, J. Rossbach, E. Plönjes, and M. Drescher, Nat. Photonics **3**, 523 (2009).
[41] J. Ullrich, R. Moshammer, A. Dorn, R. Dörner, L. Ph. H. Schmidt, and H. Schmidt-Böcking, Rep. Prog. Phys. **66**, 1463 (2003).
[42] A. Kramida, Yu. Ralchenko, J. Reader, and NIST ASD Team, Nist at. spect. database (ver. 5.0), 2013.
[43] J. J. Yeh and I. Lindau, At. Data Nucl. Data Tables **32**, 1 (1985).
[44] For example, $(^1\mathrm{S})3p(^2\mathrm{P})$ at 59.43 eV, $(^1\mathrm{D})3d(^2\mathrm{P})$ at 59.46 eV, $(^1\mathrm{D})3d(^2\mathrm{S})$ at 59.51 eV, $(^3\mathrm{P})4d(^2\mathrm{P})$ at 59.14 eV, $(^3\mathrm{P})4d(^2\mathrm{D})$ at 59.06 eV, and $(^3\mathrm{P})4p(^2\mathrm{P})$ at 58.05 eV [36].
[45] P. A. Heimann, U. Becker, H. G. Kerkhoff, B. Langer, D. Szostak, R. Wehlitz, D. W. Lindle, T. A. Ferrett, and D. A. Shirley, Phys. Rev. A **34**, 3782 (1986).
[46] K. Schulz, M. Domke, R. Püttner, A. Gutiérrez, G. Kaindl, G. Miecznik, and C. H. Greene, Phys. Rev. A **54**, 3095 (1996).
[47] Calculated according to Refs. [11,15,18] for $\lambda = 800$ nm.
[48] $t_{\mathrm{clc}}(E) \approx -(1/E^{3/2})[\ln(4E/\omega_{\mathrm{THz}}) - \gamma_{\mathrm{E}} + (\pi\omega_{\mathrm{THz}}/8E)]$ [11], $t_{\mathrm{clc}}(E) \approx -(1/E^{3/2})\{\ln[0.37(2\pi E/\omega_{\mathrm{THz}})] - 1\}$ [15], $t_{\mathrm{clc}}(E) \approx -(1/E^{3/2})\{\ln(4E/\omega_{\mathrm{THz}}) - \gamma_{\mathrm{E}} - 1 + [3\pi\omega_{\mathrm{THz}}/4(2E)^{3/2}]\}$ [18].
[49] M. Ossiander, F. Siegrist, V. Shirvanyan, R. Pazourek, A. Sommer, T. Latka, A. Guggenmos, S. Nagele, J. Feist, J. Burgdörfer, R. Kienberger, and M. Schultze, Nat. Phys. **13**, 280 (2017).